Article:
Nazir, R, Parida, D, Guex, AG et al. (8 more authors) (2020) Structurally Tunable pH-responsive Phosphine Oxide Based Gels by Facile Synthesis Strategy. ACS Applied Materials and Interfaces, 12 (6). pp. 7639-7649. ISSN 1944-8244

https://doi.org/10.1021/acsami.9b22808

Structurally tunable pH-responsive phosphine oxide based gels by facile synthesis strategy

Rashid Nazir[a], Dambarudhar Parida[a], Anne Géraldine Guex[b], Daniel Rentsch[c], Afsaneh Zarei[d], Ali Gooneie[a], Khalifah A Salmeia[a], Kevin M. Yar[a], Farzaneh Alihosseini[d], Amin Sadeghpour[e], Sabyasachi Gaan[a]**

[a] Laboratory of Advanced Fibers, Empa, Swiss Federal Laboratories for Materials Science and Technology, Lerchenfeldstrasse 5, CH-9014 St. Gallen, Switzerland

[b] Laboratory for Biointerfaces and Laboratory for Biomimetic Membranes and Textiles, Empa, Swiss Federal Laboratories for Materials Science and Technology, Lerchenfeldstrasse 5, CH-9014 St. Gallen, Switzerland

[c] Laboratory for Functional Polymers, Empa, Swiss Federal Laboratories for Materials Science and Technology, Überlandstrasse 129, 8600 Dübendorf, Switzerland.

[d] Department of Textile Engineering, Isfahan University of Technology, Isfahan, 84156-83111, Iran.

[e] Center for X-Ray Analytics, Empa, Swiss Federal Laboratories for Materials Science and Technology, Lerchenfeldstrasse 5, CH-9014 St. Gallen, Switzerland

Keywords: Phosphorus, pH-sensitive gel, Michael addition, SAXS, drug release

Abstract. Design and synthesis of nanostructured responsive gels have attracted increasing attention, particularly in the biomedical domain. Polymer chain configurations and nanodomain sizes within the network can be used to steer their functions as drug carriers. Here, a catalyst free facile one-step synthesis strategy is reported for the design of pH-responsive gels and controlled structures in nanoscale. Transparent and impurity-free gels were directly synthesized from trivinylphosphine oxide (TVPO) and cyclic secondary diamine monomers via Michael addition polymerization under mild conditions. NMR analysis confirmed the consumption of all TVPO and the absence of side products, thereby eliminating post purification steps. The small angle X-ray scattering (SAXS) elucidates the nanoscale structural features in gels, i.e., it demonstrates the presence of collapsed nanodomains within gel networks and it was possible to tune the size of these domains by varying the amine monomers and the nature of the solvent. The fabricated gels demonstrate structure tunability via solvent-polymer interactions and pH specific drug release behavior. Three different anionic dyes (Acid Blue 80, Acid Blue 90 and Fluorescein) of varying size and chemistry were incorporated into the hydrogel as model drugs and their release behavior was studied. Compared to in acidic pH, a higher and faster release of Acid Blue 80 and Fluorescein was observed at pH 10, possibly due to their increased solubility in alkaline pH. In addition, their release kinetics in phosphate buffered saline (PBS) and simulated body fluid (SBF) matrix was positively influenced by the ionic interaction with positively charged metal ions. In case of hydrogel containing Acid blue 90 a very low drug release (<1%) was observed which is due to the reaction of its accessible free amino group with the vinyl groups of the TVPO. In vitro evaluation of the prepared hydrogel using human dermal fibroblasts indicates no cytotoxic effects, warranting further research for biomedical applications. Our strategy of such gel synthesis lay the basis for the design of other gel based functional materials.

1. Introduction

Design of gels with controlled nanostructures and response to external stimuli such as pH,[1-4] temperature,[5, 6] light[7], ionic strength[8, 9], enzyme[10], chemical[11] and combinations of these[11] has received increasing attention for applications in biomedical, smart actuators and material sciences.[12-18] Smart gels can be synthesized from polymers via noncovalent crosslinking[19] or covalent crosslinking.[20] Even though noncovalent gels have better response time in many applications, covalently crosslinked controlled synthesis is preferred due to the enhanced mechanical properties of gels.[21-23] However, the drawback of such gels is the presence of residual monomers, crosslinkers, or catalysts which impose further complications, i.e. sophisticated post purification steps particularly needed when biomaterials design and the living tissues are involved.[5, 24] Moreover, uncontrolled crosslinking can result in non-reproducible optical and mechanical properties.[5, 25] Reaction mechanisms like Diels-Alder and Michael addition reaction having site-specific reactivity and thermal sensitivity can be alternative synthetic strategies in such situations to achieve cleaner gels with tunable structures and functions.[26-28] Wei et al. highlighted the usefulness of Diels-Alder reaction to prepare hydrogels from poly(ethylene glycol) dienophile and polymeric diene.[26, 27, 29] More recently, Wang et al. synthesized antimicrobial hydrogels by incorporating antimicrobial poly-carbonate chains by Michael addition reaction.[28]. In most cases where Michael addition reaction has been used to synthesize gels, a catalyst has been used and their removal from final product is not addressed. [30-36] Additionally, gels prepared by these means also involve multiple steps of post-modification and purification.[19, 37-41] Developing gelators with site-specific reactivity is essential to eliminate multiple intermediate steps and achieve cleaner gels. The nanoscale architectural features, e.g. the chain configurations and network homogeneity, induce varying diffusion rates for the loaded drugs in gels.[42] Therefore, the tunable network

structures offer new opportunities for fabrication of polymer gels with drug delivery applications.[43-45]

Herein we report a new single-step strategy for the synthesis of clean and transparent gels with tunable nanoscale network structure. Catalyst free Michael addition reactions between vinyl groups of trivinylphosphine oxide (TVPO) and diamines were conducted (Figure 1a) under a controlled solvent-polymer interaction. A pH-responsive hydrogel was designed by an appropriate selection of diamine backbones which leads to a controlled drug release behavior. Compared to the reactant monomers alone, a reduced cytotoxic effect was demonstrated for the developed hydrogel. This underlines that a high purity and complete gelation has been achieved in a one-step synthesis procedure. Thus, the synthesized gels show a great potential as a drug carrier and can be used in other biomedical applications.

2. Experimental Section

2.1. Materials and Methods

Phosphoryl trichloride, vinyl magnesium bromide (1M in THF), dry THF, 1,6-dibromohexane, 1,10-dibromodecane, 1,3-di(piperidin-4-yl)propane, piperazine, piperidine, tert-butyl piperazine-1-carboxylate (1), cyanuric chloride (6), Acid blue 90, Acid blue 80 and Fluorescein were obtained from Aldrich and used as received unless otherwise stated. The compounds trivinylphosphine oxide (TVPO),[46] 1,6-di(piperazin-1-yl)hexane (3),[47] 1,10-di(piperazin-1-yl)decane (5)[47] were synthesized via modified procedures (SI section S2) and 2,4,6-tri(piperazin-1-yl)-1,3,5-triazine (8)[48] was synthesized using procedure as described in the literature.

2.2. NMR analysis

The ^{1}H, ^{13}C and ^{31}P NMR spectra and the ^{1}H, ^{13}C 2D correlation experiments were recorded using the Bruker standard pulse programs on a 5 mm CryoProbe™ Prodigy probe equipped with z-gradient applying 90° pulse lengths of 11.4 µs (^{1}H), 10.0 µs (^{13}C) and 16.0 µs (^{31}P) on a Bruker AV-III 400 NMR spectrometer (Bruker Biospin AG, Fällanden, Switzerland). ^{1}H NMR data are reported as follows: chemical shift, numbers of protons contributing to the signal intensity, multiplicity (s = singlet, d = doublet, t = triplet, q = quartets, m = multiplet, br = broad), coupling constants (*J* in Hz) and assignment to chemical structure. For ^{13}C NMR data multiplicities s = quaternary carbon, *d* = CH, t = CH_2, and *q* = CH_3 are shown. The ^{31}P NMR chemical shifts were referenced to an external sample with neat (phosphoric acid) H_3PO_4 at 0.0 ppm. ^{1}H and ^{13}C NMR chemical shifts were referenced to the residual solvent signals at 7.26 and 77.0 ppm for (deuterated chloroform) $CDCl_3$, 4.79 for (deuterium oxide) D_2O and 3.31 and 49.0 ppm for (deuterated methanol) CD_3OD, respectively. The ^{13}C NMR data in D_2O solution was referenced to an external sample of 3-(trimethylsilyl)-2,2,3,3-tetradeuteropropionic acid (TMSP) at 0.0 ppm. Gels were analyzed by using "gel-phase-NMR," by synthesizing them directly in deuterated solvents in NMR tubes. Interpretation of all gels was performed via 1D and 2D NMR spectroscopy.

2.3. Synthesis of hydrogel (Gel-A)

A mixture of TVPO (64.0 mg, 0.50 mmol) and piperazine (64.6 mg, 0.75mmol) in water (2.5 mL) was taken in a glass vial and sealed. The vial was then transferred to an oven preheated at 60 °C for 1h, affording **Gel-A** as a transparent hydrogel. ^{1}H NMR (400.2 MHz, D_2O) δ (ppm): 2.79 (m, H-a); 2.63 (m, H-β1, β2); 2.49 (m (br), H-b, c); 2.09 (m, H-α). ^{13}C NMR (100.6 MHz, D_2O) δ

(ppm): 52.1 (t, C-b); 51.1 (t, C-c); 49.7 & 49.1 (t, C-β1, β2); 43.9 (t, C-a); 23.7 (dd, J_{CP} = ca. 63 Hz, C-α [-CHD-]). ^{31}P NMR (162.0 MHz, D_2O) δ (ppm): 54.5-55.1.

Synthesis of tris(2-(piperidin-1-yl)ethyl)phosphine oxide (9)

In a glass pressure tube (Ace pressure tube, bushing type, back seal, volume ~15 mL, L × O.D. 10.2 cm × 25.4 mm) in heating blocks on a hot plate a mixture of TVPO (64.0 mg, 0.50 mmol) and piperidine (127.7 mg, 1.5 mmol) were added to methanol (2.5 mL). The resulting mixture was stirred at 50 °C for 2 hours; the solvent was evaporated and the residue dried under vacuum to afford compound 9 with 98% (189 mg) yield. ^{1}H NMR (400.2 MHz, CD_3OD) δ (ppm): 2.65 (m, 6H, H-β); 2.48 (m (br), 12H, H-a); 2.10 (m, 6H, H-α); 1.62 (m, 12H, H-b); 1.49 (m, 6H, H-c). ^{13}C NMR (100.6 MHz, CD_3OD) δ (ppm): 55.1 (t, C-a); 52.2 (t, C-β); 26.7 (t, C-b); 26.5 (td, J_{CP} = 64.7 Hz, C-α); 25.2 (t, C-c). ^{31}P NMR (162.0 MHz, CD_3OD) δ (ppm): 52.1.

Synthesis of tris(2-(piperidin-1-yl)ethyl)phosphine oxide (9-D) in CD_3OD.

In a NMR glass tube a mixture of TVPO (12.8 mg, 0.1 mmol) and piperidine (29.8 mg, 0.35 mmol) were added to CD_3OD (0.7 mL). The resulting mixture was hated at 50 °C in pre-heated oven for 2 hours and NMR data recorded without any further workup.

^{1}H NMR (400.2 MHz, CD_3OD) δ (ppm): 2.75 (m, 4H, H-a of piperidine); 2.65 (m, 6H, H-β); 2.48 (m (br), 12H, H-a); 2.10 (m, 6H, H-α [-CH_2-]); 2.07 (m, 3H, H-α [-CHD-]); 1.7-1.6 (m, 6H, H-b,c of piperidine); 1.62 (m, 12H, H-b); 1.49 (m, 6H, H-c). ^{13}C NMR (100.6 MHz, CD_3OD) δ (ppm): 55.1 (t, C-a); 52.2 (t, C-β); 47.6 (t, C-a of piperidine); 27.4 (t, C-b of piperidine); 26.7 (t, C-b); 26.5 (td, J_{CP} = 64.6 Hz, C-α [-CH_2-]); 26.2 (dd, J_{CP} = 64.6 Hz, J_{CD} = 19.4 Hz, C-α [-CHD-]); 25.8 (t, C-c of piperidine); 25.2 (t, C-c).

2.4. Rheology of gels

The gelation reaction of the monomer solution was monitored on a rotational rheometer (MCR 301, Anton Paar, Austria) in situ at a set temperature of 40 °C. Parallel plate geometry was utilized with a plate diameter of 43 mm and an initial gap of 200 µm. The gap thickness was controlled automatically to minimize the normal forces due to possible swelling or shrinkage of the sample during the gelation. The time sweeps were carried out at a constant strain and frequency of 0.1% and 10 Hz, respectively. In-situ gelation of monomers from solution was carried out under a rotational rheometer. By measuring the storage modulus G' as a function of time, we are able to probe the gelation reaction as it proceeds. The equilibrium crosslink densities ν were estimated using the relation $G_0 = \nu k_B T$ with the storage modulus at low frequencies G_0, the Boltzmannconstant k_B, and the reaction temperature T.[49]

2.5. Solvent affinity of gels (swelling behavior).

The swelling behavior of synthesized gels were studied in solvents with different polarities for example water (polar protic, dielectric constant (ε) = 80.1), ethanol (polar protic, ε = 24.5), dichloromethane (polar aprotic, ε = 8.9) and toluene (polar protic, ε = 2.38). The swelling ratio (SR) of gels were determined by soaking the gels in solvents for 24 hours, removed from the solvent and weighed after removing the excess solvent from the surface with a moist tissue paper. The swelling ratio (SR) of the gel were calculated according to equation Eq-S1 in Sec. S4. In the case of the pH-sensitive hydrogel, the swelling ratio was determined at different pH (22 ºC) following the procedure described above. The desired pH was achieved by the addition of 0.1 N HCl and 0.1 N NaOH solution.

2.6. SEM analysis of Gel-A

SEM analysis of Gel-A was carried out in a Hitachi S-4800 SEM operating at 20 kV. Prior to SEM analysis, freeze-dried **Gel-A** samples (dimensions approx. 20 mm × 50 mm) were prepared under different pH values.

2.7. Small-angle X-ray scattering (SAXS)

SAXS measurements were done in a Bruker Nanostar instrument (Bruker AXS GmbH, Karlsruhe, Germany) equipped with a micro-focus copper radiation (CuKα 1.5406 Å) source. More details about SAXS setup is provided elsewhere.[50] The scattering profiles have been recorded at the sample-detector distance of 107 cm providing the reliable q-range between 0.06 to 2.2 nm-1 ($q = (4\pi/\lambda) \sin(\theta)$, where 2θ is the scattering angle). The samples were measured inside quartz capillaries of 1.5 mm outer diameter and the wall thickness of 0.1 mm (Hilgenberg GmbH, Malsfeld, Germany). The profiles were corrected for background subtraction taking into account the transmission signal from all samples as well as empty capillary and the one filled with the solvent (a new home-designed and built semi-transparent beam stop was mounted which allowed a dedicated and precise background subtraction). The capillaries were wax-sealed and the measurement chamber were evacuated (to 0.1 mbar) prior to measurement to reduce the air scattering. All experiments were performed at room temperature (22 °C).

2.8. Drug release from hydrogel (Gel-A)

To study the drug release behavior, three different anionic dyes (Figure S42) were incorporated into the hydrogel (**Gel-A**) via the in-situ upload method which ensures full (100%) incorporation

of dyes in the gels. For each drug release test, a solution was prepared with the TVPO (2 mmol), Piperazin (3 mmol) and the drug (20 mg) in 10 ml deionized water. Dyes were initially dissolved in water at room temperature prior to the addition of TVPO and piperazine. Then the solution was transferred to a vial and the vial was transferred to an oven at 60 °C to prepare the hydrogel. Subsequently, the gels were washed with water and immersed in the release solutions at different pH and release behaviors of the gels were monitored via UV-VIS spectrophotometer. HCl and NaOH were used to prepare acidic and basic solutions while phosphate buffer was used for pH 7. 4. In addition, the release behavior of dyes in simulated body fluid was also determined. The calibration curve was prepared for dye concentration range between 0.001-0.05 mg/mL. The limit of detection (LOD) was evaluated as the dye concentration in which the peak produced a signal-to-noise ratio greater > 10. The percentage of released dye per amount of initial dye loaded in the gel was measured and reported.

2.9. Cytotoxicity of the hydrogel (Gel-A)

Cell culture - Normal human dermal fibroblasts (NHDF, PromoCell, C-29910, Germany) were expanded and cultured in Dulbecco's Modified Eagle Medium, high glucose (DMEM, Sigma-Aldrich, Switzerland), supplemented with 10% v/v fetal calf serum, 1% Glutamine, and 1% Penicillin, Streptomycin, Neomycin (PSN) (all from Invitrogen, Thermo Fisher Scientific, Switzerland). NHDF were seeded at a density of 5000 cells per well in 96-well plates (Techno Plastic Products (TPP), Switzerland) (~5700 cells·cm-^{2}) and let to adhere overnight. Subsequently, 100 µL conditioned media was added to each well, and cell culture maintained at 37 °C, 5% CO_2 for up to three days.

Preparation of conditioned media - Cytotoxicity of the hydrogels was assessed by use of conditioned media by following the ISO Norm 10993-5. The hydrogels were directly prepared in 15 mL falcon tubes. After gelation, hydrogels were sterilized in 10% v/v PSN in PBS on a rotating shaker. Subsequently, serum-free DMEM at a 10 % v/v ratio hydrogel to DMEM was added to the tubes, followed by incubation for 24 hours at 37 °C and 5% CO_2 in a humidified incubator. As a control, DMEM without hydrogel was aged under the same condition. Prior to addition to the cells, DMEM was supplemented with 10% FCS; fresh DMEM served as a standard, while DMEM supplemented with 0.1 % v/v Triton-X 100™ was used as the cytotoxic, cell-lysing control. Following the same approach, the monomers TVPO and piperazine were also assessed in a preliminary test at concentrations of 10% v/v in DMEM (N=1 individual experiment, n=3 replicates).

Cell viability assay and DNA quantification - On day 1 and day 3, cell metabolic activity was assessed via an alamarBlue assay (ThermoFisher Scientific, Switzerland). NHDF were incubated with a 10% v/v solution of alamarBlue in phenol-red free DMEM for 2 hours. Fluorescence intensity was measured on a Mithras^2 Plate reader (Berthold Technologies, Germany) at λ_{ex}=540 nm and λ_{em} = 580 nm. NHDF were then washed in PBS and lysed in MilliQ water in three repeated freezing-thawing cycles.

DNA of lysed cells was quantified with a Hoechst DNA quantification assays, based on a fluorescent DNA binding agent (bis-benzimidazole, Hoechst 33258, Sigma, Switzerland). Fluorescence intensity was quantified at λ_{ex}=350 nm and λ_{em} = 460 nm and normalized to a standard curve of calf thymus DNA. Light microscopy images were acquired on a Zeiss Primovert (Zeiss GmbH, Germany).

All experiments were accomplished with n=3 replicates per condition in N=5 (alamarBlue) or N=4 (Hoechst) independent experiments. Statistical significance was assessed with GraphPad Prism6 based on pairwise comparisons in a non-parametric Mann-Whitney test. Differences of the mean were accepted as significant for $p<0.05$.

3. Results and Discussion

Detailed synthesis and characterization of TVPO, diamines and gels are described in the supplementary information (SI). The gels were synthesized in a simple single-step method using TVPO and diamines (1:1 molar ratio) and labeled as **Gel-A** to **E** (Figure 1a). We observed an increase in the gelation time from 1 hour in the case of **Gel-A** to 24 hours for **Gel-D** and **Gel-E** (Figure 1a).

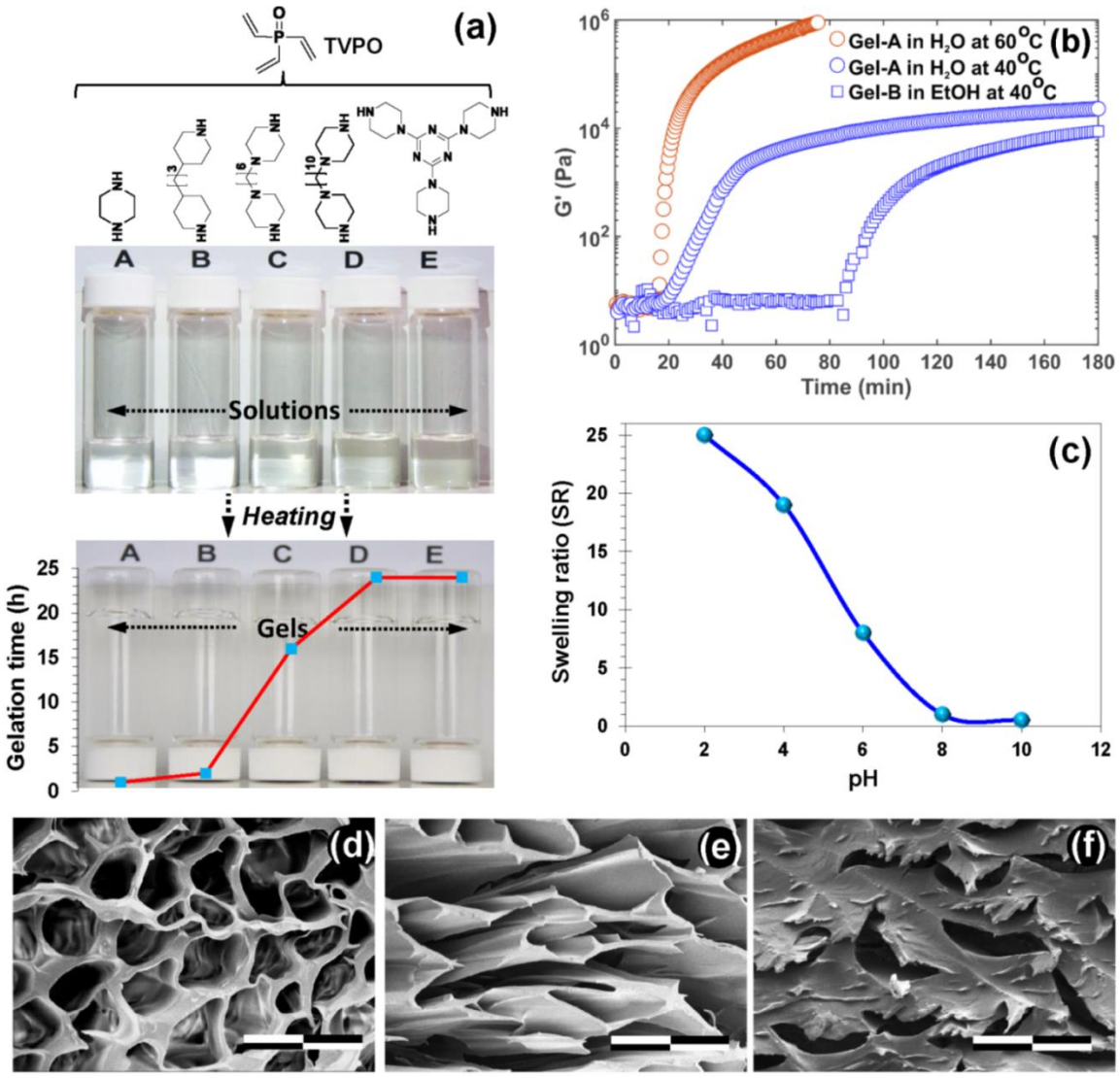

Figure 1. (a) Synthesis of phosphorus-based gels from TVPO and different diamines at 60 ºC in ethanol. Graph (red) shows the gelation time for different gels **A-E** at 60 °C, **(b)** Gelation time of **Gel-A** at (40 °C and 60 °C in water) and of **Gel-B** (40°C in ethanol) determined by rheometry. For comparison, the gelation time of Gel-B was determined and was found to be higher than **Gel-A**. **(c)** The Swelling ratios of hydrogel (**Gel-A**) at different pH (swelling ratio <1 refers to the de-swelling of **Gel-A**). The procedure and calculation of swelling ratio can be found in the supplementary information (S4). **(d)**, **(e)** and **(f)** are showing the SEM images of **Gel-A** at pH 4, 7 and 10 respectively. Scale bar in SEM images: 100 µm.

Such positive correlation between gelation time and molecular size of amines can be attributed to reduced diffusion of long amine chains. The effects of temperature and structure of diamines on gelation time was confirmed by in-situ synthesis of **Gel-A** and **Gel-B** by rotational rheometry (Figure 1b). At lower temperature (40 °C), **Gel-A**formed with a longer gelation time (~ 60 min) as compared to the much faster gelationof ~ 20 min at a higher temperature (60 °C). The crosslink densities of **Gel-A** in water and Gel-B in ethanol are ~14.3 and ~8.0 mol/m^3, respectively. These estimations agree well with the typical ν values of hydrogels between ~5-50 mol/m^3 reported in the literature.[21, 51-54] From figure 1b, it can be clearly seen that gel (**Gel-B**) synthesized with a longer amine requires longer gelation time (120 min). These findings are in agreement with our visual observations. The obtained gels were colorless and transparent, independent of the type of amines backbones and gelation time, giving firsthand information about the controlled reaction. This observation confirms the absence of visible light multiple scattering which could originate from domains of chain aggregates in microscale or larger scale. Interestingly, the gelation reaction was specific only to cyclic secondary diamines. No gels were obtained in case when linear aliphatic primary or secondary amines were used as monomers, even after prolonged heating. This can be attributed possible cyclization reactions that impedes polymerization.[55] The low-temperature gelation under cross-linker/catalyst-free condition and amine specific reactivity is a quite unique feature, enabling formulations to incorporate thermosensitive molecules or reagents.[30]

Alkyl chain lengths between piperidine and piperazine units of diamines was found to alter the hydrophilicity of the gels (Figure S17). The use of piperazine led to the formation of a hydrogel differing in comparison to the hydrophobic gels obtained for amines with longer alkyl bridge (**Gel-B** to **Gel-E**). The polar amino groups in the gel network and dipole-dipole interactions of polar

phosphoryl groups favors maximum swelling in polar aprotic solvents like dichloromethane (DCM) compared to polar protic counterparts (e.g. ethanol), [19] while inhibiting swelling in a non-polar solvent such as toluene (Figure S17). The hydrogel was found to be pH-responsive with a maximum swelling ratio of 25 at pH 2, whereas deswelling was observed at pH 10 (Figure 1c). SEM analysis of freeze-dried **Gel-A** (Figure 1 d-f) at different pH values confirmed the pH responsiveness of the materials. At pH 4 an open structure with uniformly distributed pores are observed (Figure 1d), which decreases with increasing pH values and finally collapses at pH 10 (Figure 1f). SEM analysis is in well agreement with pH-responsive swelling of **Gel-A**. Swelling at low pH can be attributed to the intramolecular electrostatic repulsions of protonated amines in acidic medium. Partial deprotonation of amines in basic medium leads to de-swelling of the gels.[56]

As pre-synthesized gels could not be homogeneously transferred into NMR tubes, gels for the NMR studies were synthesized directly in a deuterated solvent and analyzed in situ with "gel phase NMR". The chemical assignments of ^{1}H and ^{13}C NMR resonances for all gels were performed via 1D and 2D NMR spectroscopy (detailed summary for all gels are described in SI, paragraph S5). In the case of **Gel-A**, the almost complete absence of the olefinic protons characteristic of TVPO at 5.8-6.4 ppm (Figure 2a) was observed, implying that the vinyl groups of the starting material were consumed to > 99% (Figure 2b, ^{1}H NMR spectrum with integrated regions shown in Figure S18). For the methylene group labeled with "α" in the chemical structure of **Gel-A** (Figure 2b) a cross signal with the opposite sign of signal intensity can be observed in the multiplicity-edited HSQC NMR spectrum (Figure 3b) compared to the relative signal intensities of all other CH_2 groups in the molecule. Therefore, this correlation must originate from a CH (or CH_3) carbon. Since the polymerization reaction follows a Michael addition type mechanism and therefore a CH_2 group is expected at position α, separate model reactions were performed using piperidine as amine

ligand in i) normal methanol, resulting in compound **9** and ii) in deuterated methanol which results in compound **9-D**. Thorough analysis of the NMR data reveals that in the ^{13}C NMR spectrum of compound **9** the signal for C-α [-CH_2-] at 26.5 ppm splits into a doublet (J_{CP} = 64.6 Hz) (Figure S22). These two resonances are present also in the ^{13}C NMR data of compound **9-D**, but an additional set of resonances can be assigned to a –CHD-group at 26.2 ppm (α position) split into a doublet by J_{CP} = 64.6 Hz and a 1:1:1 triplet due to the coupling with deuterium incorporated by reaction with deuterium from the solvent (J_{CD} = 19.4 Hz, Figure S23 and S24).

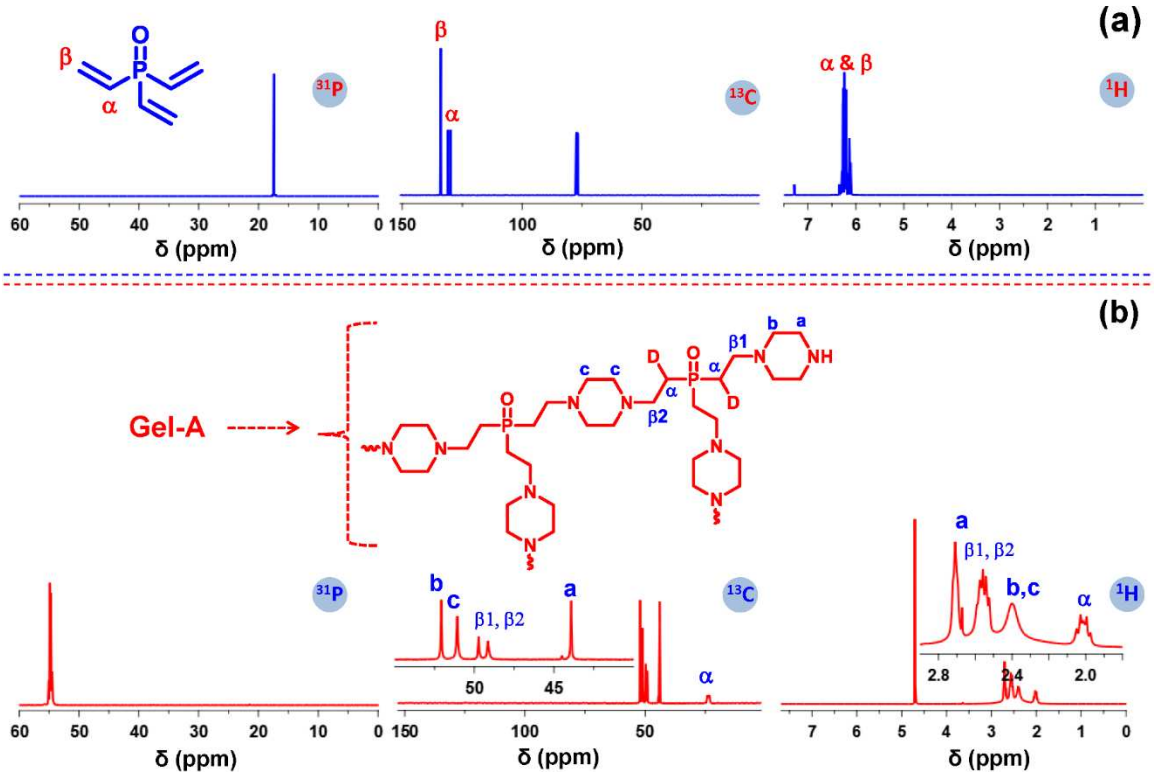

Figure 2. (a) ^{1}H, ^{13}C, ^{31}P NMR spectra of TVPO in $CDCl_3$, **(b)** ^{1}H, ^{13}C, ^{31}P NMR spectra of **Gel-A** showing shifts in corresponding peaks as a confirmation of reaction (D_2O).

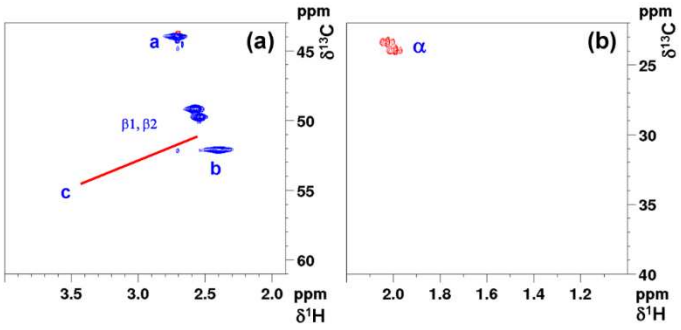

Figure 3. (a, b) expanded regions of ^{1}H-^{13}C HSQC NMR spectrum with assigned cross peaks of **Gel-A** (D_2O). The red line points to the missing correlation signal of positions c.

Coming back to the HSQC NMR data of **Gel-A**, the cross signal at 2.09 / 23.7 ppm (Figure 3a) therefore was assigned to a –CHD- group (position α). The two peaks around 2.63 / δ 49.7 ppm belong to position β, bound either to piperazine with only one attached phosphorous ligand with cross peaks of the amine moiety at 2.49 / 43.9 ppm (position a) and 2.49 / δ 52.1 ppm (position b), or to a piperazine unit with two phosphorous ligands attached ($\delta^{13}C$ of 51.1 ppm, position c, see Figure 2b). No correlation to this carbon is detectable in the HSQC NMR spectrum (indicated by red line in Figure 3) and in the DEPT-135 NMR spectrum (Figure S19), a signal of only minor intensity is observed. Both pulse sequences operate with a polarization transfer from ^{1}H to ^{13}C and do not seem to work properly due to the limited mobility in the gel phase associated with line broadening (with short T_2 relaxation as a consequence) of ^{1}H NMR resonances. Finally, the assignment of carbon c to a methylene group via the APT NMR pulse sequence was possible (Figure S19, multiplicity selection in APT experiments is based on ^{13}C magnetization dephasing during a delay without polarization transfer). In addition, the completeness of consumption of

TVPO vinyl groups was documented by the disappearance of the ^{31}P NMR signal at 17.4 ppm (Figure 2a) and the simultaneous build-up of resonances at δ 54.5-55.1 ppm (Figure 2b).

To further elucidate the nanostructure of the gels small-angle X-ray scattering (SAXS) technique was used. Initially, we observed that the scattering intensity for **Gel-A** and **Gel-C** (Figure 4a) decays with characteristics value for 3-dimensional domains (Porod slope of -4). The 3-D domains also formed in **Gel-D** but with much smaller size confirmed by initial plateau at the scattering profile followed by the decay at large q values. Kratky plots (I×q2 versus q) provide more detailed information on polymer chains behavior in the gels (Figure 4b); we observe maxima at q values.

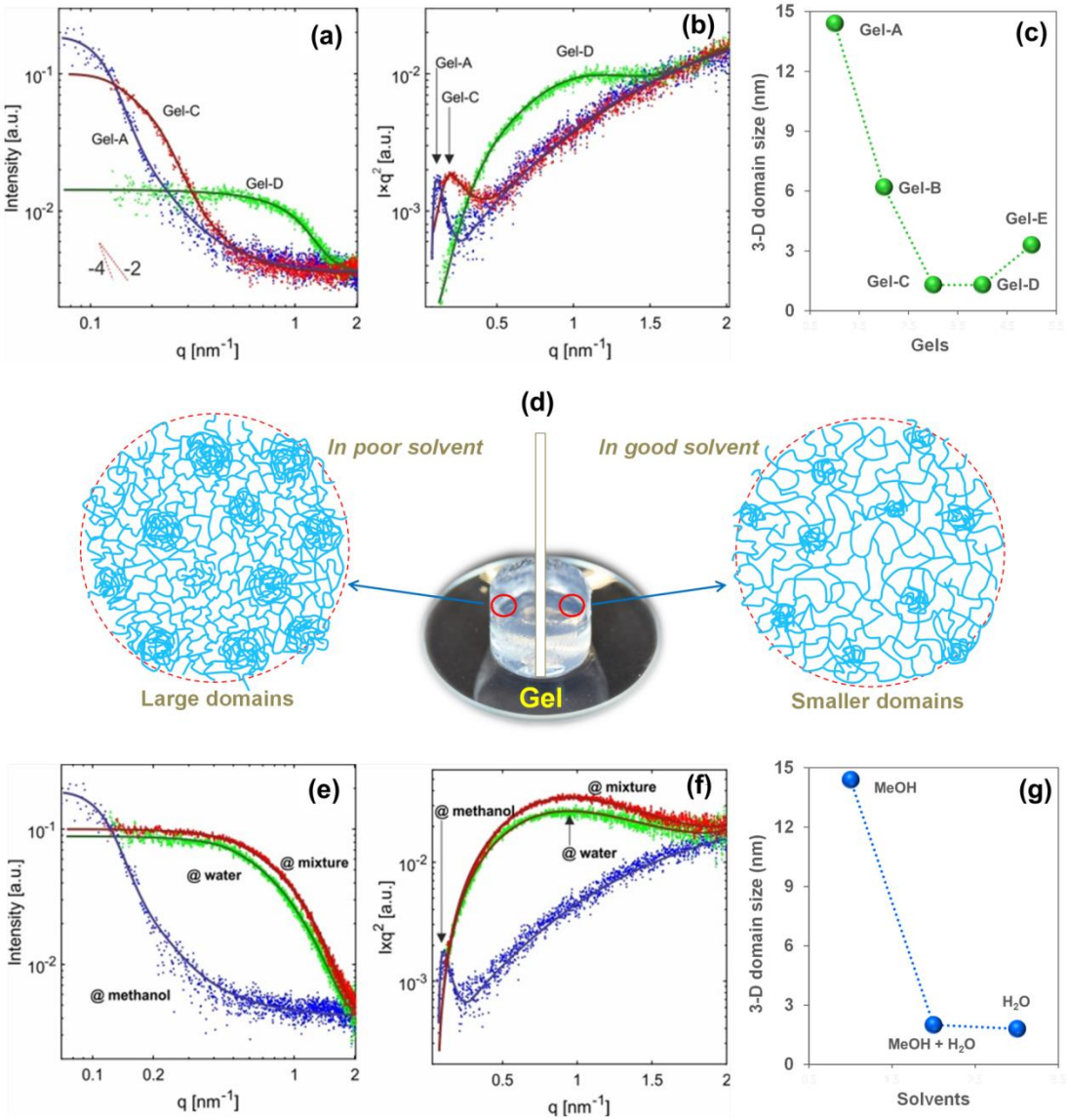

Figure 4. **(a) (b)** the Kratky plots of gels prepared with diamines bearing varying hydrocarbon chains, **(c)** size of nano domains formed based on the hydrocarbon chain length of amine and its compatibility with the solvent (methanol), **(d)** Proposed microstructure of these gels, showing changes in the size of nano domains with respect to different solvents. **(e, f)** Scattering profiles and the Kratky plots of hydrogel prepared in H_2O, methanol and H_2O-methanol mixture (1:1). **(g)** Change in size of collapsed domains present in the hydrogel in different solvent compositions.

This may be due to increased compatibility between polymer chains and methanol owing to increased hydrophobicity of longer hydrocarbon chain length of diamines. From SAXS studies, it can be deduced that the large collapsed polymer domains can be achieved in gels synthesized in poor solvents whereas domain formation was suppressed when a favorable solvent is used. Such scattering behavior for conformational changes of macromolecules has been demonstrated in numerous studies previously. [57-60] The schematic presentation of structural variations in different gels is shown in figure 4d.

To validate the influence of solvent compatibility on nano-domains formation, **Gel-A**, which exhibits the largest collapsed domain in methanol, was synthesized in different water-methanol composition. Due to higher solvent compatibility, **Gel-A** is expected to have extended chain conformation in water or smaller domain size. SAXS Kratky plot of **Gel-A** in water (Figure 4f) shows the disappearance of a sharp maxima at 0.11 nm^{-1} and the appearance of a plateau with a shallow peak around 1.0 nm^{-1}. The plateau confirms polymer chain configuration with Gaussian behavior in water compared to that in methanol nevertheless, a small fraction of collapsed chain cannot be excluded due to the presence of the shallow peak.[61] Using Guinier fit (Figure S37 and S38), we could quantify the domain sizes of 2.0 nm in water, which is far smaller compared to 14 nm domain size in methanol (Figure 4g). Noteworthy that the **Gel-A** in 1:1 water/methanol mixture also shows similar behavior to the polymer in pure water (Figure 4e, 4f).

Gel-B and **Gel-E** have been synthesized from monomers of slightly different structures, however, the nanostructure can still be tuned by the strategy based on solvent compatibility. Gel-B contains two piperidine rings connected via a propyl group, which is expected to have a higher hydrophobicity compared to **Gel-E** with three piperazine groups. As a result, the **Gel-B** shows monotonous increase indicating solely elongated chains in contrast to **Gel-E** which demonstrates

a shallow peak in Kratky plot. (See Figure S39, S40 and S41). The Ornstein-Zernike modeling of **Gel-B** in methanol reveals about 1.3 nm correlation length along the stretched polymer chain. [62] For the **Gel-E** in methanol, the domain sizes of 3.3 nm is demonstrated by a shallow peak in the Kratky plot at around 0.5 nm^{-1} (Figure S41).

Motivated by the clean and pH-responsive nature of the phosphorous hydrogel, their drug release potential was evaluated using three different model drugs like Acid blue 80, Acid Blue 90 and Fluorescein (Figure S42). These drugs were carefully chosen to demonstrate the effect of dye molecular weight (Acid Blue 90- MW 854, Acid Blue 80- MW 678 and Fluorescein- MW 332) on release behavior and their possible reaction of the amine group of these dyes with the gel network. Acid Blue 90 and Acid Blue 80 have free secondary amino groups, which can potentially react with vinyl groups of TVPO. The secondary amino group in Acid Blue 80 is sterically hindered and may not be readily available for reaction with the vinyl group of TVPO. In contrast, Fluorescein is relatively a small anionic dye with no amino group and thus expected to exhibit a different release profile. Hydrogels (**Gel-A)** loaded with the model drug (dyes) were prepared via the in-situ loading method. The in-situ drug loading method involved mixing of the dye solution with the monomers followed by hydrogel synthesis. This process ensures 100 % incorporation of all inside the gel. To ascertain any possible side reaction between dye and hydrogel matrix, UV-vis spectra of dye solution (in water) and dye loaded hydrogels were recorded by preparing the dye loaded hydrogel directly inside UV-cuvettes. From figure S43a, S47a it can be seen that UV-vis absorption peaks of hydrogel bound Acid blue 80 and Fluorescein remained identical to their solution, indicating the absence of any kind of reaction between dye and hydrogel. Such a shift can be attributed to possible reactions between -NH group of Acid blue 90 and vinyl group of TVPO. This was further confirmed by a longer gelation time (3 h) when the in-situ loading of Acid

blue 90 was carried out. To confirm the reaction between dye molecules and hydrogel matrix, reaction between TVPO and Acid blue 90 was carried out by heating in D_2O at 60 °C for 1 hour (Figure S45). The ^{31}P NMR revealed the appearance of additional phosphorous peaks confirming the reaction between TVPO and Acid blue 90 (Figure S45). Whereas, no change in ^{31}P NMR spectra was observed when a mixture of TVPO and Acid blue 80 was heated at 60 °C for 1 hour (Figure S44). Subsequently, all dye-loaded hydrogels were investigated for their release behavior.

Despite a swollen state of the hydrogel below pH 6, an exhibition of a very slow drug release profile (Figure 5a) can be attributed to the strong interaction between the anionic dye and cationic hydrogel. Such interactions with drug molecules have already been reported as a release control strategy in polymer networks.[63] At higher pH(10), a faster release kinetics (up to 14%) possibly due to increased solubility of acid blue 80 in alkaline pH and the reduced pore size of the hydrogel matrix was observed. When dye release was investigated in a phosphate buffer solution (pH 7.4), a faster kinetics with the controlled-release pattern was observed compared to the release kinetics at higher pH (Figure 5a). Release kinetics in PBS and SBF after 24 hours is positively influenced by the ionic affinity between positively charged metal ions and the anionic dye, thus playing a crucial role in a higher releasing rate.[64] Such release behavior can be utilized in injuries, where pH changes from neutral or basic pH (~10) are observed,[65] thus acting as a trigger for the release of active ingredients encapsulated within the hydrogel.

Acid blue 90, comparatively a higher molecular weight dye was loaded in the hydrogel and its release was studied in different solutions. Acid blue 90 exhibited the lowest release rate (Figure 5b) and this is due to the reaction of TVPO and secondary amines of dye which inhibits its subsequent release (Figure S45).

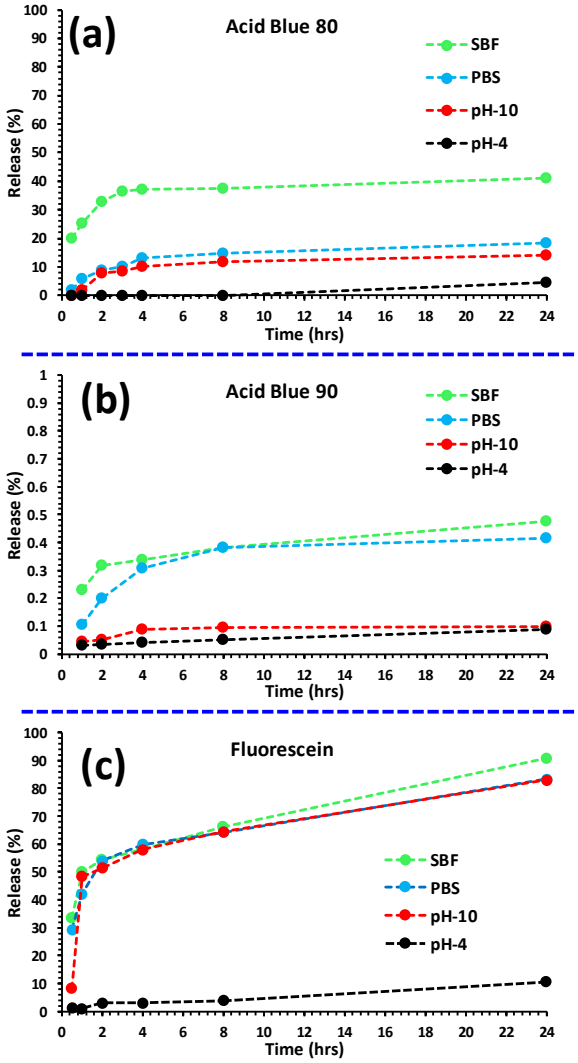

Figure 5: (a) Kinetics of Acid Blue 80, **(b)** Acid Blue 90 **(C)** and Fluorescein release from **Gel-A** in simulated body fluid (SBF), PBS buffer and at different pH.

Fluorescein loaded hydrogel exhibited slightly different release behavior compared to the other dye/hydrogel systems. Unlike in case of Acid Blue 80 loaded hydrogel, a small release of Fluorescein (up to 10 %) is observed in acidic media (at pH 4) %) (Figure 5c) which may be due

to its small size and swollen state of the hydrogel. However, the poor release of Fluorescein in acidic media could be attributed to e to protonation of its carboxylic group which makes it more hydrophobic compared to its deprotonated form in an alkaline media. In contrast, at a higher pH (10), a faster release of Fluorescein was observed (up to 70%) possibly due to higher solubility of the dye in alkaline media. The release rate of Fluorescein in PBS is higher and comparable to that in alkaline media due to the ionic affinity between positively charged metal ions present in PBS and the negatively charged groups of the dye. Compared to PBS, in SBF, a higher and faster release of Fluorescein (up to 90 % after 24hrs) was observed which may be due to a high concentration of metal ions (Figure 5c).

To exclude the potential metal complexation of the dyes (Acid blue 80 and Fluorescein), their UV spectra in different media were measured and provided in figures S43, S47. As , no change in λ_{max} of Acid Blue 80 in variousmedia was observed, it possible metal complexation can be excluded. Similarly, for Fluorescein (Figure S47), no change in λ_{max} was observed in all media except in pH 4. In acidic pH (4) values, the λ_{max} of Fluorescein was shifted to lower wavenumber (Figure S47b) which is due to its cationic structure.[66]

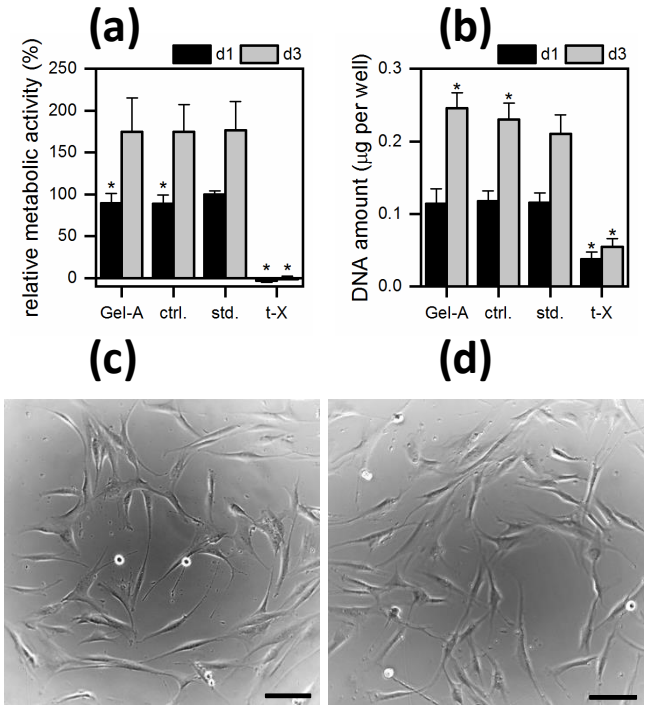

Figure 6. (a) Cell metabolic activity of normal human dermal fibroblasts (NHDF) on day 1 (d1) and day 3 (d3) based on an alamar Blue assay. Values are normalized to NHDF cultured in fresh DMEM (std.) on d1. DMEM incubated at 37°C for 24h without **Gel-A** served as control (ctrl.), triton –X-100^{TM} supplemented DMEM as cytotoxic condition (t-X). N=5 individual experiments, **(b)** DNA amount, an estimate for cell number, was quantified based on a Hoechst assay. N=4 individual experiments. *$p<0.05$ compared to std. of the same day. **(c)** and **(d)** light microscopy images of NHDF cultured on tissue culture plastic (TCP), treated with **(c)** fresh DMEM (std.) and **(d) Gel-A** extracts. Scale bar: 10 µm.

Cytotoxicity of **Gel-A** (hydrogel) was assessed based on extract exposure (cell culture media incubated with the material of interest) of normal human dermal fibroblasts (NHDF). This is a

versatile pilot test and gives the first indication of the suitability of a material for biomedical application. Potentially toxic and soluble substances could alter the metabolic activity of cells and/or affect their proliferation rate. Cytotoxicity assays were performed based on ISO 10993-5, postulating that a cell metabolic activity of <70% compared to a standard control group indicates a cytotoxic effect of the material extracts.

In a first preliminary evaluation (results presented in Figure S48), the two reactants piperazine and TVPO were evaluated. At concentrations of 10% v/v in DMEM, both monomers had a cytotoxic effect, indicated by relative cell metabolic activities lower than 70% compared to fresh DMEM. In consecutive experiments, the materials were evaluated after gelation (**Gel-A** formation). Conditioned media (**Gel-A**), as well as media incubated at 37°C for 24 h without the addition of **Gel-A** (ctrl.) did reduce the metabolic activity of NHDF compared to cells cultured in fresh media (std.) on day 1. Importantly, however, the relative metabolic activity was higher than 80% compared to NHDF cultured under standard conditions (Figure 6a). This indicates that in the chosen in vitro model of human dermal fibroblasts, extracts of the prepared hydrogels did not have a cytotoxic effect. Reduced cell metabolic activity in these two groups (**Gel-A** and ctrl.) can be attributed to reduced nutrient content in media incubated for 24 hours at 37°C rather than a cytotoxic impact of **Gel-A**. No significant differences in cell metabolic activity among the three groups were observed on day 3which is also in favor of the assumption that **Gel-A** is cytocompatible. DNA quantities of **Gel- A** extract-treated cells were comparable to the standard group (std.) on day 1, while statistically significantly higher values were found on day 3 for both groups (**Gel-A** and ctrl.) compared to std. (Figure 6b). Hoechst is a DNA intercalating agent, which also stains the DNA of dead cells remaining in the culture well. This explains the relatively high values for Triton -X-100™ treated cells, as well as the discrepancy between cell metabolic activity

and DNA quantity. Cytotoxicity assays, as well as microscopical observations point in the same direction, indicating that **Gel-A** extracts did not have a cytotoxic effect on NHDF. Compared to the observed cytotoxic effect the two monomers (piperazine and TVPO) have on NHDF (Figure S 48), these results are further in favor of fast, complete gelation of the here synthesized hydrogel. Even though the ISO 10993-5 norm has been developed as a standard to assess medical devices, the experimental design described therein provides versatile guidelines for initial evaluations of various (bio)materials to assess potentially cytotoxic extractable. Confirmed cytocompatibility then warrants further research on the newly synthesized or developed material. Further in-depth evaluations, in particular with drug-loaded hydrogels in specific in vitro model systems are needed to elucidate the potential use of the here designed hydrogel as a drug delivery matrix for medical application.

4. Conclusion

A facile one-step strategy for the synthesis of phosphine oxide based gels under mild conditions is reported in this work. Gel phase NMR study (1D and 2D NMR spectroscopy) was used to characterize the structure of gels. Only Michael addition products in the form of phosphine oxide macromolecules were identified in the NMR study. SAXS analysis was used to investigate the nanostructure of the gels and it was able to detect the presence of collapsed nanodomains within the microstructure of the gels. Three anionic dyes (Acid Blue 90, Acid Blue 80, and Fluorescein) as model drugs were loaded in hydrogel (**Gel-A**) via an in-situ method. In alkaline medium, Acid Blue 80 and Fluorescein were released faster from the hydrogel which is due to increased solubility of the dyes. A higher and faster release of these dyes was observed in PBS and SBF which is due to the ionic interaction of metal ions present in these media. In case of Acid Blue 90 a very low

release was observed in various media which is due to the reaction of its easily accessible secondary amino group with the vinyl group of TVPO. Thus, this work demonstrates that the chemical structure and the molecular weight of the dye, pH of the media and the composition of the release media (PBS and SBF) influence the dye release rate from the hydrogel. As-synthesized hydrogel (**Gel-A**) without further purification was subjected to cytotoxicity assessment. In vitro cytotoxic assessment of **Gel-A** using human dermal fibroblasts did not show any cytotoxic effect. These properties indeed make these gels promising candidates for drug delivery matrix and other biomedical applications.

5. Associated content

Supporting Information. The Supporting Information is available free of charge on the ACS Publications website.

Synthesis and NMR characterization of diamines; ^{1}H, ^{13}C, ^{31}P and HSQC NMR data of gels; SAXS scattering profiles and corresponding Guinier fits of **Gel-A**, **Gel-C** and **Gel-D**; detailed procedure for swelling ratio determination, drug release behavior, cytotoxicity assessment are given in supporting information.

AUTHOR INFORMATION

Corresponding Authors

*E-mail: sabyasachi.gaan@empa.ch

*E-mail: amin.sadeghpour@empa.ch

Funding Sources

SNSF grant IZSEZ0_182882 and Zürcher Stiftung für Textilforschung (project number 116)

Notes

Authors declare no conflicting interests.

6. Acknowledgment

The authors acknowledge SNSF grant IZSEZ0_182882 for partially funding this project. The NMR hardware was partially granted by the Swiss National Science Foundation (SNSF, grant no. 206021_150638/1). The Authors also acknowledge Zürcher Stiftung für Textilforschung (project number 116) for partially funding the project.

REFERENCES

1. Cinay, G. E.; Erkoc, P.; Alipour, M.; Hashimoto, Y.; Sasaki, Y.; Akiyoshi, K.; Kizilel, S., Nanogel-Integrated Ph-Responsive Composite Hydrogels for Controlled Drug Delivery. *ACS Biomaterials Science & Engineering* **2017,** *3* (3), 370-380.
2. Dao, H. M.; Chen, J.; Tucker, B. S.; Thomas, V.; Jun, H.-W.; Li, X.-C.; Jo, S., Hemopressin-Based Ph-Sensitive Hydrogel: A Potential Bioactive Platform for Drug Delivery. *ACS Biomaterials Science & Engineering* **2018,** *4* (7), 2435-2442.
3. Ruan, H.; Hu, Q.; Wen, D.; Chen, Q.; Chen, G.; Lu, Y.; Wang, J.; Cheng, H.; Lu, W.; Gu, Z., A Dual-Bioresponsive Drug-Delivery Depot for Combination of Epigenetic Modulation and Immune Checkpoint Blockade. *Advanced Materials* **2019,** *31* (17), 1806957.
4. Gačanin, J.; Hedrich, J.; Sieste, S.; Glaßer, G.; Lieberwirth, I.; Schilling, C.; Fischer, S.; Barth, H.; Knöll, B.; Synatschke, C. V.; Weil, T., Autonomous Ultrafast Self-Healing Hydrogels by Ph-Responsive Functional Nanofiber Gelators as Cell Matrices. *Advanced Materials* **2019,** *31* (2), 1805044.
5. Jin, C.; Song, W.; Liu, T.; Xin, J.; Hiscox, W. C.; Zhang, J.; Liu, G.; Kong, Z., Temperature and Ph Responsive Hydrogels Using Methacrylated Lignosulfonate Cross-Linker: Synthesis, Characterization, and Properties. *ACS Sustainable Chemistry & Engineering* **2018,** *6* (2), 1763-1771.
6. Matsumoto, K.; Sakikawa, N.; Miyata, T., Thermo-Responsive Gels That Absorb Moisture and Ooze Water. *Nature Communications* **2018,** *9* (1), 2315.
7. Muraoka, T.; Koh, C.-Y.; Cui, H.; Stupp, S. I., Light-Triggered Bioactivity in Three Dimensions. *Angewandte Chemie International Edition* **2009,** *48* (32), 5946-5949.

8. van Bommel, K. J. C.; van der Pol, C.; Muizebelt, I.; Friggeri, A.; Heeres, A.; Meetsma, A.; Feringa, B. L.; van Esch, J., Responsive Cyclohexane-Based Low-Molecular-Weight Hydrogelators with Modular Architecture. *Angewandte Chemie International Edition* **2004,** *43* (13), 1663-1667.
9. Kim, H.-J.; Lee, J.-H.; Lee, M., Stimuli-Responsive Gels from Reversible Coordination Polymers. *Angewandte Chemie* **2005,** *117* (36), 5960-5964.
10. Ma, D.; Zhang, L.-M.; Xie, X.; Liu, T.; Xie, M.-Q., Tunable Supramolecular Hydrogel for in Situ Encapsulation and Sustained Release of Bioactive Lysozyme. *Journal of Colloid and Interface Science* **2011,** *359* (2), 399-406.
11. Bowerman, C. J.; Nilsson, B. L., A Reductive Trigger for Peptide Self-Assembly and Hydrogelation. *Journal of the American Chemical Society* **2010,** *132* (28), 9526-9527.
12. Ballios, B. G.; Cooke, M. J.; van der Kooy, D.; Shoichet, M. S., A Hydrogel-Based Stem Cell Delivery System to Treat Retinal Degenerative Diseases. *Biomaterials* **2010,** *31* (9), 2555-2564.
13. Tan, H.; Ramirez, C. M.; Miljkovic, N.; Li, H.; Rubin, J. P.; Marra, K. G., Thermosensitive Injectable Hyaluronic Acid Hydrogel for Adipose Tissue Engineering. *Biomaterials* **2009,** *30* (36), 6844-6853.
14. Kraehenbuehl, T. P.; Ferreira, L. S.; Zammaretti, P.; Hubbell, J. A.; Langer, R., Cell-Responsive Hydrogel for Encapsulation of Vascular Cells. *Biomaterials* **2009,** *30* (26), 4318-4324.
15. Sá-Lima, H.; Caridade, S. G.; Mano, J. F.; Reis, R. L., Stimuli-Responsive Chitosan-Starch Injectable Hydrogels Combined with Encapsulated Adipose-Derived Stromal Cells for Articular Cartilage Regeneration. *Soft Matter* **2010,** *6* (20), 5184-5195.
16. Culver, H. R.; Clegg, J. R.; Peppas, N. A., Analyte-Responsive Hydrogels: Intelligent Materials for Biosensing and Drug Delivery. *Accounts of Chemical Research* **2017,** *50* (2), 170-178.
17. Ono, T.; Sugimoto, T.; Shinkai, S.; Sada, K., Lipophilic Polyelectrolyte Gels as Super-Absorbent Polymers for Nonpolar Organic Solvents. *Nature Materials* **2007,** *6*, 429.
18. Hoffman, A. S., Hydrogels for Biomedical Applications. *Advanced Drug Delivery Reviews* **2012,** *64*, 18-23.
19. Roy, S. G.; Kumar, A.; De, P., Amino Acid Containing Cross-Linked Co-Polymer Gels: Ph, Thermo and Salt Responsiveness. *Polymer* **2016,** *85*, 1-9.
20. Kato, S.; Aoki, D.; Otsuka, H., Introducing Static Cross-Linking Points into Dynamic Covalent Polymer Gels That Display Freezing-Induced Mechanofluorescence: Enhanced Force Transmission Efficiency and Stability. *Polymer Chemistry* **2019**.
21. Xia, Z.; Patchan, M.; Maranchi, J.; Elisseeff, J.; Trexler, M., Determination of Crosslinking Density of Hydrogels Prepared from Microcrystalline Cellulose. *Journal of Applied Polymer Science* **2013,** *127* (6), 4537-4541.
22. Truong, V. X.; Ablett, M. P.; Richardson, S. M.; Hoyland, J. A.; Dove, A. P., Simultaneous Orthogonal Dual-Click Approach to Tough, in-Situ-Forming Hydrogels for Cell Encapsulation. *Journal of the American Chemical Society* **2015,** *137* (4), 1618-1622.
23. Zhou, Y.; Damasceno, P. F.; Somashekar, B. S.; Engel, M.; Tian, F.; Zhu, J.; Huang, R.; Johnson, K.; McIntyre, C.; Sun, K.; Yang, M.; Green, P. F.; Ramamoorthy, A.; Glotzer, S. C.; Kotov, N. A., Unusual Multiscale Mechanics of Biomimetic Nanoparticle Hydrogels. *Nature Communications* **2018,** *9* (1), 181.

24. Ahmed, E. M., Hydrogel: Preparation, Characterization, and Applications: A Review. *Journal of Advanced Research* **2015,** *6* (2), 105-121.
25. N. A. Peppas; Y. Huang; M. Torres-Lugo; J. H. Ward, a.; Zhang, J., Physicochemical Foundations and Structural Design of Hydrogels in Medicine and Biology. *Annual Review of Biomedical Engineering* **2000,** *2* (1), 9-29.
26. Wei, H.-L.; Yang, J.; Chu, H.-J.; Yang, Z.; Ma, C.-C.; Yao, K., Diels–Alder Reaction in Water for the Straightforward Preparation of Thermoresponsive Hydrogels. *Journal of Applied Polymer Science* **2011,** *120* (2), 974-980.
27. Wei, H.-L.; Yang, Z.; Chu, H.-J.; Zhu, J.; Li, Z.-C.; Cui, J.-S., Facile Preparation of Poly(N-Isopropylacrylamide)-Based Hydrogels Via Aqueous Diels–Alder Click Reaction. *Polymer* **2010,** *51* (8), 1694-1702.
28. Liu, S. Q.; Yang, C.; Huang, Y.; Ding, X.; Li, Y.; Fan, W. M.; Hedrick, J. L.; Yang, Y.-Y., Antimicrobial and Antifouling Hydrogels Formed in Situ from Polycarbonate and Poly(Ethylene Glycol) Via Michael Addition. *Advanced Materials* **2012,** *24* (48), 6484-6489.
29. Wei, H. L.; Feng, Y. L.; Chu, H. J.; Yao, K., Fabrication of Supramolecular Structured Hydrogels Based on Diels-Alder Click Reaction. *Advanced Materials Research* **2012,** *562-564*, 405-408.
30. Vermonden, T.; Censi, R.; Hennink, W. E., Hydrogels for Protein Delivery. *Chemical Reviews* **2012,** *112* (5), 2853-2888.
31. Lee, B. H.; West, B.; McLemore, R.; Pauken, C.; Vernon, B. L., In-Situ Injectable Physically and Chemically Gelling Nipaam-Based Copolymer System for Embolization. *Biomacromolecules* **2006,** *7* (6), 2059-2064.
32. Robb, S. A.; Lee, B. H.; McLemore, R.; Vernon, B. L., Simultaneously Physically and Chemically Gelling Polymer System Utilizing a Poly(Nipaam-Co-Cysteamine)-Based Copolymer. *Biomacromolecules* **2007,** *8* (7), 2294-2300.
33. Wang, Z.-C.; Xu, X.-D.; Chen, C.-S.; Yun, L.; Song, J.-C.; Zhang, X.-Z.; Zhuo, R.-X., In Situ Formation of Thermosensitive Pnipaam-Based Hydrogels by Michael-Type Addition Reaction. *ACS Applied Materials & Interfaces* **2010,** *2* (4), 1009-1018.
34. Lutolf, M. P.; Tirelli, N.; Cerritelli, S.; Cavalli, L.; Hubbell, J. A., Systematic Modulation of Michael-Type Reactivity of Thiols through the Use of Charged Amino Acids. *Bioconjugate Chemistry* **2001,** *12* (6), 1051-1056.
35. Hahn, S. K.; Oh, E. J.; Miyamoto, H.; Shimobouji, T., Sustained Release Formulation of Erythropoietin Using Hyaluronic Acid Hydrogels Crosslinked by Michael Addition. *International Journal of Pharmaceutics* **2006,** *322* (1), 44-51.
36. Lutolf, M. P.; Hubbell, J. A., Synthesis and Physicochemical Characterization of End-Linked Poly(Ethylene Glycol)-Co-Peptide Hydrogels Formed by Michael-Type Addition. *Biomacromolecules* **2003,** *4* (3), 713-722.
37. Cheng, J.; Zhang, P.; Liu, T.; Zhang, J., Preparation and Properties of Hydrogels Based on Peg and Isosorbide Building Blocks with Phosphate Linkages. *Polymer* **2015,** *78*, 212-218.
38. Wang, Y.; Li, L.; Kotsuchibashi, Y.; Vshyvenko, S.; Liu, Y.; Hall, D.; Zeng, H.; Narain, R., Self-Healing and Injectable Shear Thinning Hydrogels Based on Dynamic Oxaborole-Diol Covalent Cross-Linking. *ACS Biomaterials Science & Engineering* **2016,** *2* (12), 2315-2323.
39. Zhang, L.; Jeong, Y.-I.; Zheng, S.; Kang, D. H.; Suh, H.; Kim, I., Crosslinked Poly(Ethylene Glycol) Hydrogels with Degradable Phosphamide Linkers Used as a Drug Carrier in Cancer Therapy. *Macromolecular Bioscience* **2014,** *14* (3), 401-410.

40. Zhang, L.; Choi, E. J.; Kim, M. H.; Lee, G. M.; Suh, H.; Kim, I., Ph-Reversible Supramolecular Hydrogels Based on Aminoalkyl Phosphoamide Compounds. *Supramolecular Chemistry* **2012,** *24* (3), 189-196.
41. Liu, Z.; Wang, L.; Bao, C.; Li, X.; Cao, L.; Dai, K.; Zhu, L., Cross-Linked Peg Via Degradable Phosphate Ester Bond: Synthesis, Water-Swelling, and Application as Drug Carrier. *Biomacromolecules* **2011,** *12* (6), 2389-2395.
42. Walker, C. N.; Versek, C.; Touminen, M.; Tew, G. N., Tunable Networks from Thiolene Chemistry for Lithium Ion Conduction. *ACS Macro Letters* **2012,** *1* (6), 737-741.
43. Qin, L.; Xie, F.; Duan, P.; Liu, M., A Peptide Dendron-Based Shrinkable Metallo-Hydrogel for Charged Species Separation and Stepwise Release of Drugs. *Chemistry – A European Journal* **2014,** *20* (47), 15419-15425.
44. Matson, J. B.; Newcomb, C. J.; Bitton, R.; Stupp, S. I., Nanostructure-Templated Control of Drug Release from Peptide Amphiphile Nanofiber Gels. *Soft Matter* **2012,** *8* (13), 3586-3595.
45. Chen, Y.; Gao, Y.; da Silva, L. P.; Pirraco, R. P.; Ma, M.; Yang, L.; Reis, R. L.; Chen, J., A Thermo-/Ph-Responsive Hydrogel (Pnipam-Pdma-Paa) with Diverse Nanostructures and Gel Behaviors as a General Drug Carrier for Drug Release. *Polymer Chemistry* **2018,** *9* (29), 4063-4072.
46. Bisaro, F.; Gouverneur, V., Desymmetrization by Direct Cross-Metathesis Producing Hitherto Unreachable P-Stereogenic Phosphine Oxides. *Tetrahedron* **2005,** *61* (9), 2395-2400.
47. Zhang, R.; Wu, X.; Yalowich, J. C.; Hasinoff, B. B., Design, Synthesis, and Biological Evaluation of a Novel Series of Bisintercalating DNA-Binding Piperazine-Linked Bisanthrapyrazole Compounds as Anticancer Agents. *Bioorganic & Medicinal Chemistry* **2011,** *19* (23), 7023-7032.
48. Chouai, A.; Venditto, V. J.; Simanek, E. E.; McDermott, R. E.; Ragan, J. A., Synthesis of 2-[3,3'-Di-(Tert-Butoxycarbonyl)-Aminodipropylamine]-4,6,-Dichloro-1,3,5-Triazine as a Monomer and 1,3,5-[Tris-Piperazine]-Triazine as a Core for the Large Scale Synthesis of Melamine (Triazine) Dendrimers. *Organic syntheses; an annual publication of satisfactory methods for the preparation of organic chemicals* **2009,** *86*, 141-150.
49. Larson, R. G., The Structure and Rheology of Complex Fluids (Topics in Chemical Engineering). *Oxford University Press, New York• Oxford* **1999,** *86*, 108.
50. Maurya, A. K.; Weidenbacher, L.; Spano, F.; Fortunato, G.; Rossi, R. M.; Frenz, M.; Dommann, A.; Neels, A.; Sadeghpour, A., Structural Insights into Semicrystalline States of Electrospun Nanofibers: A Multiscale Analytical Approach. *Nanoscale* **2019**.
51. Lee, J. H.; Bucknall, D. G., Swelling Behavior and Network Structure of Hydrogels Synthesized Using Controlled Uv-Initiated Free Radical Polymerization. *Journal of Polymer Science Part B: Polymer Physics* **2008,** *46* (14), 1450-1462.
52. Liu, Y.; Huglin, M. B., Effective Crosslinking Densities and Elastic Moduli of Some Physically Crosslinked Hydrogels. *Polymer* **1995,** *36* (8), 1715-1718.
53. Yazici, I.; Okay, O., Spatial Inhomogeneity in Poly(Acrylic Acid) Hydrogels. *Polymer* **2005,** *46* (8), 2595-2602.
54. Seetapan, N.; Wongsawaeng, J.; Kiatkamjornwong, S., Gel Strength and Swelling of Acrylamide-Protic Acid Superabsorbent Copolymers. *Polymers for Advanced Technologies* **2011,** *22* (12), 1685-1695.
55. Varnes, J. G.; Gero, T.; Huang, S.; Diebold, R. B.; Ogoe, C.; Grover, P. T.; Su, M.; Mukherjee, P.; Saeh, J. C.; MacIntyre, T.; Repik, G.; Dillman, K.; Byth, K.; Russell, D. J.;

Ioannidis, S., Towards the Next Generation of Dual Bcl-2/Bcl-Xl Inhibitors. *Bioorganic & Medicinal Chemistry Letters* **2014,** *24* (14), 3026-3033.
56. Zhang, J.; Xie, R.; Zhang, S.-B.; Cheng, C.-J.; Ju, X.-J.; Chu, L.-Y., Rapid Ph/Temperature-Responsive Cationic Hydrogels with Dual Stimuli-Sensitive Grafted Side Chains. *Polymer* **2009,** *50* (11), 2516-2525.
57. Takeshita, S.; Sadeghpour, A.; Malfait, W. J.; Konishi, A.; Otake, K.; Yoda, S., Formation of Nanofibrous Structure in Biopolymer Aerogel During Supercritical Co2 Processing: The Case of Chitosan Aerogel. *Biomacromolecules* **2019,** *20* (5), 2051-2057.
58. Ayuso-Tejedor, S.; García-Fandiño, R.; Orozco, M.; Sancho, J.; Bernadó, P., Structural Analysis of an Equilibrium Folding Intermediate in the Apoflavodoxin Native Ensemble by Small-Angle X-Ray Scattering. *Journal of Molecular Biology* **2011,** *406* (4), 604-619.
59. Bernadó, P.; Svergun, D. I., Structural Analysis of Intrinsically Disordered Proteins by Small-Angle X-Ray Scattering. *Molecular BioSystems* **2012,** *8* (1), 151-167.
60. Rambo, R. P.; Tainer, J. A., Characterizing Flexible and Intrinsically Unstructured Biological Macromolecules by Sas Using the Porod-Debye Law. *Biopolymers* **2011,** *95* (8), 559-571.
61. Beaucage, G., Small-Angle Scattering from Polymeric Mass Fractals of Arbitrary Mass-Fractal Dimension. *Journal of Applied Crystallography* **1996,** *29*, 134-146.
62. Nishikawa, K.; Kasahara, Y.; Ichioka, T., Inhomogeneity of Mixing in Acetonitrile Aqueous Solution Studied by Small-Angle X-Ray Scattering. *The Journal of Physical Chemistry B* **2002,** *106* (3), 693-700.
63. Li, J.; Mooney, D. J., Designing Hydrogels for Controlled Drug Delivery. *Nat Rev Mater* **2016,** *1* (12), 16071.
64. Lee, W.-F.; Chiu, R.-J., Investigation of Charge Effects on Drug Release Behavior for Ionic Thermosensitive Hydrogels. *Materials Science and Engineering: C* **2002,** *20* (1), 161-166.
65. Yano, K.; Hata, Y.; Matsuka, K.; Ito, O.; Matsuda, H., Experimental Study on Alkaline Skin Injuries—Periodic Changes in Subcutaneous Tissue Ph and the Effects Exerted by Washing. *Burns* **1993,** *19* (4), 320-323.
66. Wang, B.; Gao, W.; Ma, Y.; Li, D.; Wu, L.; Bi, L., Enhanced Sensitivity of Color/Emission Switching of Fluorescein Film by Incorporation of Polyoxometalate Using Hcl and Nh3 Gases as in Situ Stimuli. *RSC Advances* **2015,** *5* (52), 41814-41819.